

## ASSESSING PRE-INJECTION IN SITU ALTERATION OF WELLBORE CEMENT IN A SITE FOR CO<sub>2</sub> GEOLOGICAL STORAGE: A NUMERICAL APPROACH

Gherardi Fabrizio <sup>(1) (2)</sup>, Audigane Pascal <sup>(1)</sup>

<sup>(1)</sup> BRGM – 3, av. C. Guillemin, F-45060 - Orléans, France

<sup>(2)</sup> LE STUDIUM, Loire Valley Institute for Advanced Studies – 3D, av. de la Recherche Scientifique, F-45071 – Orléans, France  
e-mail: F.Gherardi@brgm.fr

### ABSTRACT

We present numerical simulations of isothermal reactive flow that might be induced by fluid migration at the caprock-cement interface of an idealized abandoned well, in an area being considered as a site for geological sequestration of carbon dioxide in the Paris Basin, France.

Field evidence, experimental data, and previous numerical simulations have been used to constrain the initial geochemical conditions and the hydraulic parameters of the numerical model. The calculations are aimed at identifying the mineralogical transformations likely occurring in the media before CO<sub>2</sub> injection, during operations and after the closure of the wells present in the area. Major mineralogical transformations in the cement (mainly portlandite dissolution), and moderate modifications of the initial clay-rock mineralogical assemblage (montmorillonite dissolution, and precipitation of zeolite and cement-like phases) are predicted. As a consequence of these reactions, porosity is expected to decrease in the caprock and to increase in the cement.

### INTRODUCTION

Site performance prediction is crucial for successful geological storage of CO<sub>2</sub>. The geological setting must be properly selected in order to guarantee that caprock formations overlying the storage reservoir will provide an effective seal, and that abandoned or active wells will not compromise the integrity of the seal.

CO<sub>2</sub> must be prevented from leaking in order to avoid hazards for humans, ecosystems, and groundwater. Injection-well failures or leakage through abandoned wells is of major concern in

risk assessments of CO<sub>2</sub> geological storage sites (IPCC, 2005). In particular, cement around the casing of existing wells may be deeply altered by interaction with CO<sub>2</sub>-rich fluids, compromising the efficiency of the seal over time (e.g. Celia and Bachu, 2003).

Unfortunately, the cement of abandoned wells is usually not accessible for direct inspection. Given this limitation, numerical modeling serves as a powerful means for predicting the mineralogical evolution of cement plugs during their *in situ* working life, and for assessing well integrity and leakage risk for the confining system before CO<sub>2</sub> injection.

Several research projects have been conducted and many others are still ongoing in France to investigate the potential of the Paris Basin aquifers for carbon dioxide geological storage purposes. In this framework, the assessment of sealing efficiency of storage sites emerges as a key factor in evaluating site performance, and ensuring public confidence regarding CO<sub>2</sub> storage (e.g., Fleury et al., 2007; Bildstein et al., 2009; and many others).

This paper presents some results from reactive transport simulations carried out to evaluate the mineralogical transformations likely affecting the sealing efficiency of cement plugs in a generic, abandoned wellbore within the Paris Basin. The objective of these numerical exercises is to identify the key geochemical processes controlling reactivity at the caprock-cement interface, and to verify if the isolation properties of the materials can be compromised during their pre-CO<sub>2</sub> injection lifetimes, i.e., *in situ* aging.

## MODEL SETUP

### Conceptual and geometrical model

Based on field data, we performed simulations under isothermal (75 °C), isobaric (15 MPa) and aqueous saturated conditions (SI = 1.0). Maximum simulation times have been fixed at 80 years to encompass the entire spectrum of ages for wells in the Paris Basin.

Reactive transport across the caprock-cement interface is simulated with a 1D-radial model. Both cement and caprock are assumed homogeneous. This simplification does not consider non-uniform sweep that may occur due to formation heterogeneities. Justification for a 1-D approach stems from the stagnant nature of the investigated system; preliminary flow simulations with 2D-radial geometries demonstrated that the low absolute permeability ( $\kappa$ ) values of the two media ( $\kappa$  values determined in the lab between  $10^{-20}$  to  $10^{-18}$  m<sup>2</sup>) impedes gravity-driven advection from developing in the system over the maximum considered simulation time of 80 years. In our model, solutes are then subjected to a purely diffusive transport regime, as commonly accepted for the modeling of interactions between concrete barriers and undisturbed clay rock.

In our model, the treatment of diffusion is based on Fick's First Law. A single, average tracer diffusion coefficient has been applied to all dissolved species. The effects of tortuosity and porosity on diffusivity are lumped together in a so-called effective diffusion coefficient, which in our model has an initial value of  $5 \times 10^{-11}$  m<sup>2</sup> s<sup>-1</sup> at the caprock-cement interface.

The mesh consists of 26 gridblocks with fixed thickness of 0.1 m, and has a radial extent of 2.5 m. The first 20 elements monitored for aqueous chemistry and mineralogy have internodal distances roughly between 2 and  $15 \times 10^{-2}$  m, progressively increasing along the radial direction.

### Materials

The initial porosity ( $\phi$ ) and absolute permeability ( $\kappa$ ) of cement and caprock materials have been fixed at average values measured on laboratory specimens (Table 1). The cement has been

simulated by a homogeneous porous medium having the composition of a hydrated ordinary class G cement paste. The primary mineralogical assemblage consists of predominant poorly crystalline calcium silicate hydrate phases (CSH:1.6), large amounts of portlandite and ettringite, relatively minor amounts of hydrogarnets (katoite-Si and Fe-katoite, C<sub>3</sub>FH<sub>6</sub>) and hydrotalcite, and traces of calcite (Table 2). Aggregates are not taken into consideration.

The mineralogical composition of the clay rock considered in this study (COx formation) has been thoroughly investigated by experimental methods and numerical simulations (e.g., among many others, Gaucher et al., 2004). The COx argillite is a complex mineral assemblage predominantly composed of phyllosilicates, silicates, carbonates, and S-bearing minerals. An average composition taken from the literature (Marty et al., 2009) has been used in the calculations (Table 2).

Table 1. Cement and caprock transport properties explored in the simulations (absolute permeability is in m<sup>2</sup>; values used in the “reference case simulation” are listed in the column “Ref”)

Cement	Range	Ref
$\phi$ , porosity	0.18 – 0.40	0.30
$\kappa$ , abs. permeab.	$10^{-18}$ to $10^{-20}$	$10^{-18}$
$\tau$ , tortuosity	0.001 to 0.1	0.01
Caprock	Range	Ref
$\phi$ , porosity	0.12 – 0.16	0.144
$\kappa$ , abs. permeab.	$10^{-18}$ to $10^{-20}$	$10^{-18}$
$\tau$ , tortuosity	0.001 to 0.1	0.01

Table 2. Cement and caprock mineralogical composition ( $V_f$  is the initial solid volume fraction)

Cement	$V_f$	Caprock	$V_f$
Calcite	0.006	Calcite	0.140
Ettringite	0.138	Illite-Mg	0.423
CSH:1.6	0.381	Montm-Mg-Na	0.060
Katoite-Si	0.105	Daphnite	0.010
Hydrotalcite	0.054	Quartz	0.240
C <sub>3</sub> FH <sub>6</sub>	0.055	Pyrite	0.010
Portlandite	0.261	Celestite	0.007

### Pore waters chemical composition

It is almost impossible to obtain representative pore-water samples for chemical analysis from both cement and caprock, because of their low hydraulic conductivity (Gaucher et al., 2009). The chemical composition of these pore waters was thus calculated by batch modeling (Table 3), following the same procedure outlined by Gherardi et al. (2012). Cement pore waters are markedly alkaline (pH around 11) and have relatively high total concentrations of dissolved Na, Ca, S, Si and Al. Caprock pore waters have a neutral pH (6.34), and, except for Al, higher total concentration of dissolved species compared to cement. This is mirrored by higher values of ionic strength (0.22 instead of 0.176 mol kg<sub>H2O</sub><sup>-1</sup>), and higher CO<sub>2</sub> fugacities (log  $f_{\text{CO}_2}$  = -1.08 instead of -10.3).

Table 3. Elemental chemical composition of cement and caprock pore waters used for the reference case simulation (isothermal at 75 °C). Total concentrations and Ionic Strength (IS) are in mol/kg<sub>H2O</sub>. Chemical components (or basis species) are in brackets.

Parameter	Cement	Caprock
pH	10.99	6.34
IS	0.176	0.224
log $a_{\text{O}_2}$ (as O <sub>2(aq)</sub> )	-60.0	-58.3
Ca (as Ca <sup>+2</sup> )	$1.79 \times 10^{-2}$	$2.55 \times 10^{-2}$
Mg (as Mg <sup>+2</sup> )	$4.45 \times 10^{-8}$	$1.65 \times 10^{-3}$
Na (as Na <sup>+</sup> )	$3.64 \times 10^{-2}$	$1.48 \times 10^{-1}$
K (as K <sup>+</sup> )	$3.80 \times 10^{-3}$	$6.43 \times 10^{-3}$
Fe (as Fe <sup>+2</sup> )	$1.34 \times 10^{-9}$	$1.00 \times 10^{-4}$
Si (as SiO <sub>2(aq)</sub> )	$1.51 \times 10^{-5}$	$6.22 \times 10^{-4}$
Al (as AlO <sub>2</sub> <sup>-</sup> )	$2.71 \times 10^{-5}$	$6.12 \times 10^{-9}$
Cl (as Cl <sup>-</sup> )	$3.91 \times 10^{-2}$	$1.90 \times 10^{-1}$
C (as HCO <sub>3</sub> <sup>-</sup> )	$8.53 \times 10^{-6}$	$2.92 \times 10^{-3}$
S (as SO <sub>4</sub> <sup>-2</sup> )	$2.83 \times 10^{-3}$	$9.22 \times 10^{-3}$

### Thermodynamic and kinetic data

The thermodynamic database used in this work includes log K values for aqueous and gaseous species and minerals listed in a recent version of Thermoddem (<http://thermoddem.brgm.fr/>), a thermodynamic database compiled at the French Geological Survey (BRGM). The primary source for equilibrium constants for aqueous species and minerals is the Slop98.dat database (Shock, 1998), with major improvements concerning cement minerals (Blanc et al., 2010). Kinetic rates and reactive surface areas are highly uncertain, and a coherent and complete kinetic database for all pertinent minerals is still far from being available to date. To circumvent this intrinsic limitation, we followed the same simplified approach outlined by Gherardi et al. (2012), using kinetic rates from Palandri and Kharaka (2004) and Wertz et al (2012).

### Numerical simulator

Simulations have been performed with the modular simulator TOUGHREACT (Xu et al., 2004). The modeling is based on space discretization by means of integral finite differences. Flow and reaction/transport equations are solved sequentially and non-iteratively. The chemical transport is solved on a component basis, and the resulting concentrations are substituted into the chemical reaction model. The system of chemical equations is solved on a gridblock basis by Newton-Raphson iteration. Full details on code capabilities and numerical methods are given in Xu and Pruess (2001) and Xu et al. (2006).

### RESULTS AND DISCUSSION

Concentration gradients in the chemical composition of cement and caprock pore waters (Table 3) represent the driving force for the mineralogical transformations predicted by TOUGHREACT.

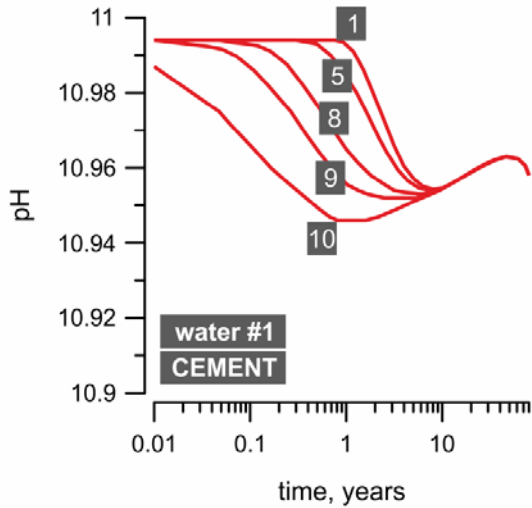


Figure 1. Temporal variation of pH for selected cells in the cement. Cement cells are labeled with numbers increasing along the radial direction, i.e. cell#1 and cell#10 are in center of the well and at the external boundary of the cement domain (i.e. at the interface with the caprock), respectively.

Most of the geochemical processes predicted by the code can be recast in terms of the competing effect between an alkaline, Al-rich plume diffusing from the cement in the caprock, and a slightly acidic, C-rich plume diffusing from the caprock in the cement. A first analysis of reaction paths is performed on the basis of pH patterns. In particular, we observe that the high buffer capacity of the cement minerals + cement pore-water system is able to maintain pH values at relatively high levels, close to the initial value of 10.99, all over the cement domain (Figure 1).

In contrast, major pH variations are predicted in the caprock. The penetration of the alkaline plume in the COx argillite is efficiently traced by a quick rise of pH values between 9 and 10.5 in the first three gridblocks of the caprock domain, and by values above 7 in the 5<sup>th</sup> cell of the caprock, at 0.4 m from the well axis, after about 38 years simulation time (Figure 2).

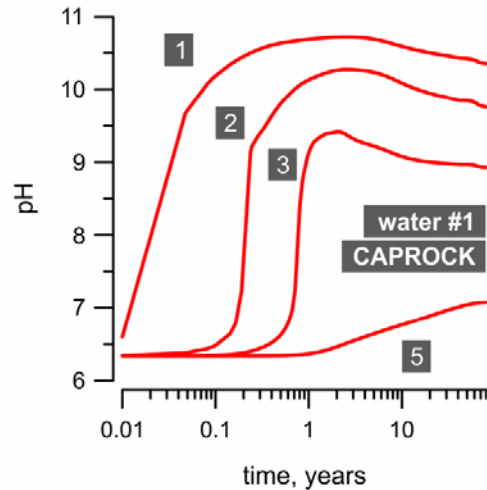


Figure 2. Temporal variation of pH for selected cells in the caprock. Caprock cells are labeled with numbers increasing along the radial direction, i.e. cell#1 is at the internal boundary of the caprock domain (i.e., at the interface with the cement).

#### Mineralogical transformations in the cement

As widely documented in the literature, most of the pH buffering predicted in the cement domain is obtained at the expenses of portlandite dissolution. Portlandite dissolves in the outermost cell of the domain, and, though at a lower extent, also in all the remaining gridblocks (Figure 3). Portlandite dissolution is an efficient marker of cement degradation, because unreacted portlandite is expected only in defect-free, unaltered cements (e.g., Glasser, 1993). The precipitation of amorphous Ca-Si gel (CSH:1.6) is another major mineralogical transformation predicted by the code (Figure 4).

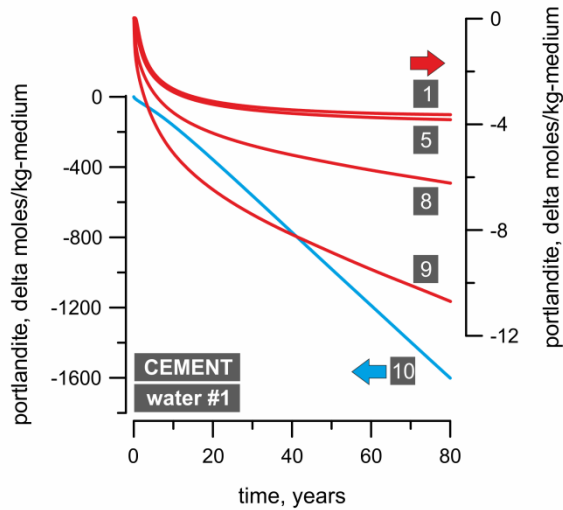


Figure 3. Temporal variation of portlandite abundance in selected cells in the cement. Labels are as in Figure 1.

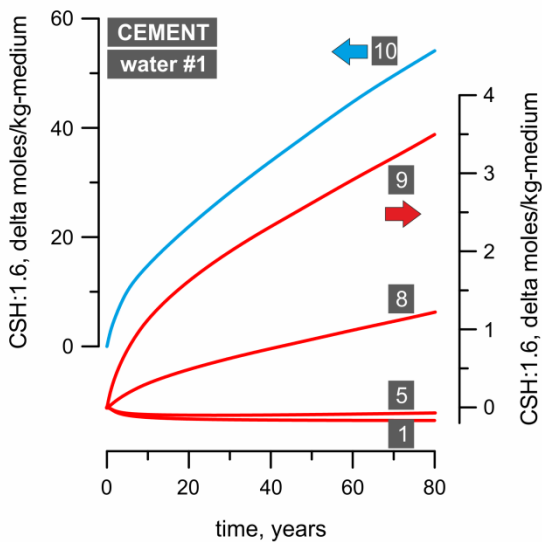


Figure 4. Temporal variation of CSH:1.6 abundance in selected cells in the cement. Labels are as in Figure 1.

The formation of secondary CSH:1.6 is accompanied by the occurrence of newly formed ettringite and hydrotalcite (first cell only). These patterns are consistent with alteration patterns commonly observed at cement-caprock interface (e.g., Gaucher and Blanc, 2006). Together with some minor calcite precipitation (secondary calcite forms in very low amounts solely in the outermost cell of the domain, close to caprock interface), these features reflect the effective buffering of total dissolved inorganic carbon

concentrations in the cement (TDIC,  $1.5 \times 10^{-5}$  mol  $\text{kg}_{\text{H}_2\text{O}}^{-1}$ ) at lower than initial caprock concentrations (caprock TDIC =  $2.92 \times 10^{-3}$  mol  $\text{kg}_{\text{H}_2\text{O}}^{-1}$ ). Low TDIC concentrations are the limiting factor controlling the level of cement carbonation.

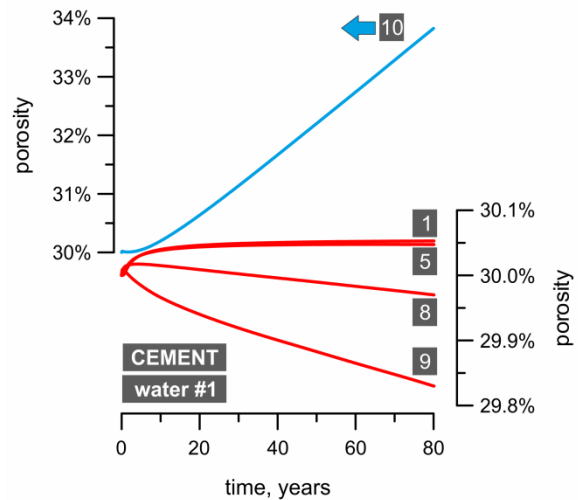


Figure 5. Temporal variation of porosity abundance in selected cells in the cement. Labels are as in Figure 1.

The massive dissolution of calcium hydroxide (portlandite) and the concomitant lack of significant carbonation has the deleterious effect of increasing the porosity in the outermost layer of the cement (about +3.8%; Figure 5), and possibly causing some loss in mechanical strength (e.g., Heukamp et al., 2001).

### Mineralogical transformations in the caprock

The overall reactivity of the caprock+cement system is controlled by the geochemical evolution of the caprock volume adjacent to cement interface. In fact, due to the mineralogical transformations occurring in this gridblock,  $\text{Ca}_{\text{TOT}}$  and TDIC concentrations steadily decrease in time (with TDIC buffered at less than  $2 \times 10^{-5}$  mol  $\text{kg}_{\text{H}_2\text{O}}^{-1}$  after 0.04 years), and virtually do not diffuse in the adjacent cement gridblocks. The mineralogical transformations predicted in the caprock are consistent with the effects of typical alkaline disturbance in clay media (e.g., Gaucher and Blanc, 2006).

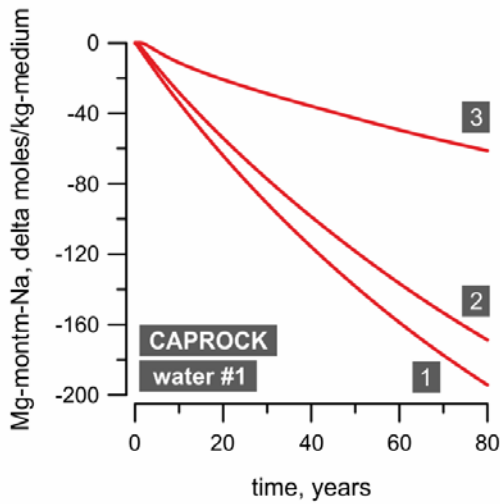


Figure 6. Temporal variation of Mg-Na-montmorillonite abundance in selected cells in the caprock. Labels are as in Figure 2.

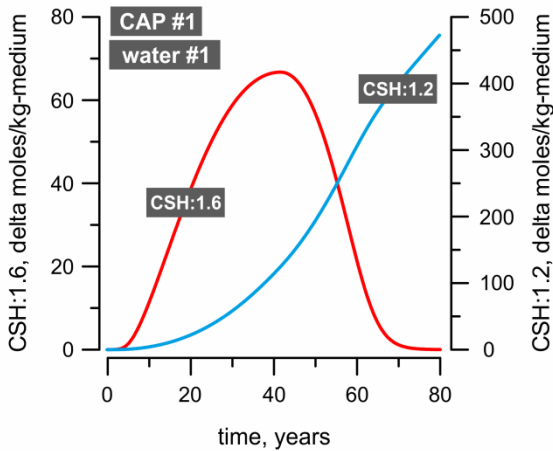


Figure 7. Temporal variation of CSH:1.6 and CSH:1.2 abundances in the first cell of the caprock domain (CAP#1), adjacent to cement interface.

The first noticeable mechanism is represented by montmorillonite destabilization (Figure 6), a process that releases important amounts of Al, Si, Mg, and Na in the aqueous solution. Other major mineralogical transformations include: precipitation of secondary illite, formation of purely cement phases (katoite, CSH:1.6, CSH:1.2; Figure 7), zeolites (K- and Ca-phillipsite; Figure 8), carbonates (calcite and hydrotalcite), chlorites, and sulfates (ettringite), dissolution of primary quartz and celestite.

Due to these reactions, porosity decreases by 3.2% in the first caprock cell adjacent to the cement interface.

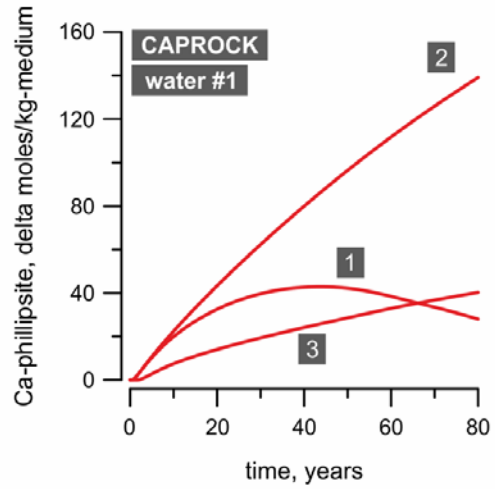


Figure 8. Temporal variation of Ca-phillipsite abundance in selected cells in the caprock. Labels are as in Figure 2.

### Sensitivity analysis

We explored the sensitivity of numerical outputs with respect to variable (i) initial chemical compositions of caprock pore waters and (ii) grid specifications.

Different chemical compositions for the CO<sub>x</sub> pore waters can be used in the model, because of the uncertainty in the equilibrium  $f_{CO_2}$  values for the argillite formation (Gaucher et al., 2009). A second water composition (water #2; Figure 9), was then computed and incorporated into the calculations to explore the effects of low- $f_{CO_2}$  initial conditions ( $\log f_{CO_2} = -2$ ) on the overall reactivity of the system. Figure 9 indicates that this water has a greater capacity to lower the pH of the cement domain. Compared to the reference-case simulation with water#1, more hydrotalcite and less calcite precipitation are now predicted in the cement, together with comparable portlandite and C<sub>3</sub>FH<sub>6</sub> dissolution rates, and ettringite precipitation rates. This behavior can be explained in terms of complex and nonlinear variations of geochemical parameters in the adjacent caprock element (less effective katoite, CSH:1.6 and CSH:1.2 precipitation, more effective calcite precipitation). Overall, the same porosity patterns of the reference-case simulation are predicted, with a

3.8% increase in the outermost cell of the cement domain (CEM#10), and a 3% decrease in the adjacent caprock gridblock (first caprock cell, CAP#1).

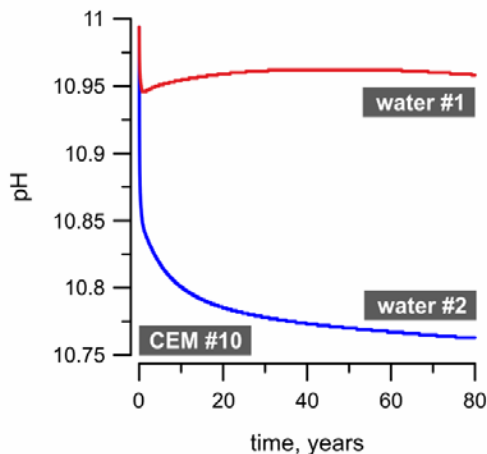


Figure 9. Temporal variation of pH in the external cell of the cement domain (CEM#10) for two different initial chemical composition of caprock pore waters.

In order to explore the effects of some hypothetically enhanced clay-rock pore-water impact on cement geochemistry, a different grid has been used with a large caprock volume set in direct contact with cement elements (“large-CAP” model). The enhanced reactivity of the cement materials now predicted by the code is mirrored by lower pH values (down to 10.88), and large variations in the mineralogical composition (Figure 10) of the outermost cell of the cement domain (CEM#10).

After 80 years simulation time, portlandite, katoite, and  $C_3FH_6$  are predicted to decrease from 26.1% to 12.3%, from 10.5% to 6.1%, and from 5.5% to 5.2% of the solid fraction of cell CEM#10, respectively. In parallel, CSH:1.6, ettringite, hydrotalcite and calcite modal abundances are predicted to increase from 38.1% to 39.5%, from 13.8 to 28.8%, from 5.4 to 6.8%, and from 0.6% to 1.3%, respectively. A major effect of this enhanced reactivity is a reverse trend in porosity compared to the reference-case simulation. Porosity clogging is in fact now predicted also in the cement, near the caprock interface, with calculated negative variations on the order of 3% after 60 years simulation time (Figure 11).

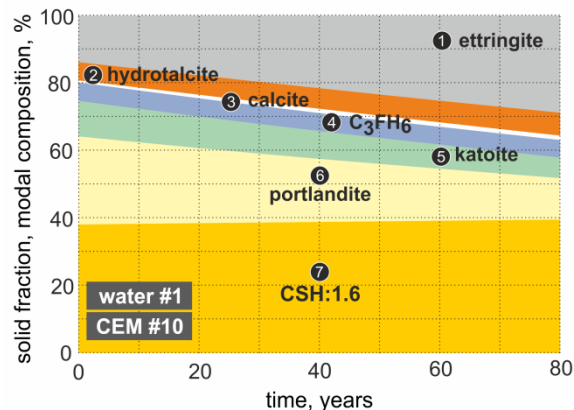


Figure 10. Mineralogical composition of the external cell of cement domain (CEM#10). Features refer to the “large CAP model.”

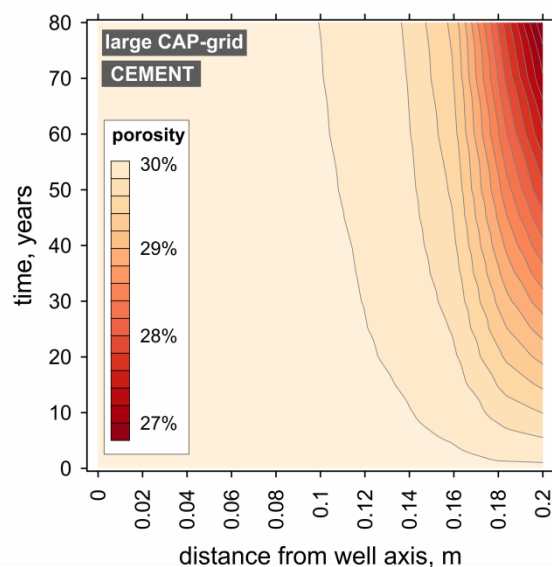


Figure 11. Contour plot showing porosity variations in the cement over 80-year simulation time. Calculations refer to the “single-large-caprock-gridblock” model.

## CONCLUSIONS

The class G cement considered in our study is subject to major degradation at pH and temperature conditions typically recognized in the Paris Basin. Together with CSH and ettringite secondary precipitation, portlandite dissolution is the main mineralogical transformation predicted in the cement. Due to the lack of significant carbonation processes, this leads to some undesired porosity enhancement near the caprock interface over the short-term simulation time (80 years) of our calculations. Based on the assumed reaction and diffusion rates, the

penetration of this alteration front is limited to the first few centimeters from caprock interface.

The rate of cement alteration is directly controlled by the geochemical transformations predicted in the adjacent caprock. In fact, due to the precipitation/dissolution processes occurring in this domain, TDIC concentrations are buffered at very low levels near the interface, preventing significant cement carbonation from occurring.

A sensitivity analysis was performed to identify the most important factors controlling the reactivity in the investigated system. Apart from the intrinsic uncertainty in the kinetic parameters and the thermodynamic characterization of field-specific mineralogical phases, the size of the caprock volume containing the infiltrating water, and the chemical composition of this water, emerged as key factors of the model. Variations in these parameters control the efficiency of calcium hydrate carbonation and porosity behavior in the cement, close to the caprock interface. Cement clogging is predicted solely under conditions of enhanced caprock pore-water penetration in the cement.

The model is an oversimplification of the processes expected under field conditions. Predictions of porosity enhancement or clogging also strongly depend on the assumption of a homogeneous distribution of hydraulic and geochemical properties in the media. More heterogeneous distributions than those numerically predicted in this work are then likely expected in reality.

## REFERENCES

- Bildstein, O., M. Jullien, A. Crédoz., and J. Garnier, Integrated modeling and experimental approach for caprock integrity, risk analysis, and long term safety assessment. *Energy Proc. 1*, 3237-3244, 2009.
- Blanc, P., X. Bourbon, A. Lassin, and E.C. Gaucher, Chemical model for cement based materials: temperature dependence of thermodynamic functions for nanocrystalline and crystalline C-S-H phases. *Cem. Concr. Res. 40*, 851–866, 2010.
- Celia, M.A., and S. Bachu, Geological sequestration of CO<sub>2</sub>: Is leakage avoidable and acceptable? *Proc 6<sup>th</sup> Int. Conf. Greenhouse Gas Control Techn.s (GHGT-6)*, Gale, J., and Y. Kaya (Eds.), Kyoto Japan, Pergamon, vol. 1, pp. 477–482, 2003.
- Fleury, M., The GeoCarbone-Integrity program: evaluating sealing efficiency of caprocks for CO<sub>2</sub> storage, GEOTECHNOLOGIEN “Science Report” No. 9: 1st French-German Symposium on Geological Storage of CO<sub>2</sub>, Abstracts from the CO<sub>2</sub>-Symposium in Potsdam, June 21-22 2007, Koordinierungsbüro Geotechnologien, p. 72, 2007.
- Gaucher E.C., and P. Blanc, Cement/clay interactions—A review: Experiments, natural analogues, and modeling. *Waste Manag. 26*, 776-788, 2006.
- Gaucher E.C., C. Tournassat, F.J. Pearson, P. Blanc, C. Crouzet, C. Lerouge, and S. Altmann, A robust model for pore-water chemistry of clayrock. *Geoch. Cosmoch. Acta 73*, 6470-6487, 2009.
- Gaucher, E.C., C. Robelin, J.M. Matray, G. Négrel, Y. Gros, J.F. Heitz, A. Vinsot, H. Rebours, A. Cassagnabère, and A. Bouchet, ANDRA underground research laboratory: interpretation of the mineralogical and geochemical data acquired in the Callovian-Oxfordian formation by investigative drilling. *Phys. Chem. Earth 29*, 55-77, 2004.
- Gherardi, F., Audigane P., and E.C. Gaucher, Predicting long-term geochemical alteration of wellbore cement in a generic geological CO<sub>2</sub> confinement site: Tackling a difficult reactive transport modeling challenge. *J. Hydrol. 420-421*, 340-359, 2012.
- Glasser, F., *Chemistry of cement solidified waste forms*, In: Chemistry and microstructure of solidified waste forms, Spence R. (ed.), Oak Ridge National Laboratory, pp. 1-39, 1993.
- Heukamp F.H., F.J. Ulm, and J.T. Germaine, Mechanical properties of calcium-leached cement pastes: triaxial stress states and the influence of pore pressures. *Cem. Concr. Res. 31*, 767–784, 2001.
- IPCC, *Carbon Dioxide Capture and Storage*, Metz B., O. Davidson, H. de Coninck, M. Loos, and L. Meyer Eds, Report prepared by the Working Group III of the Intergovern-

- mental Panel on Climate Change, Cambridge University Press, 431 pp., 2005.
- Marty, N.C.M., C. Tournassat, A. Burnol, E. Giffaut, and E.C. Gaucher, Influence of reaction kinetics and mesh refinement on the numerical modelling of concrete/clay interactions. *J. Hydrol.* 364, 58-72, 2009.
- Palandri, J.L., and Y.K. Kharaka, *A compilation of rate parameters of water-mineral interaction kinetics for application to geochemical modeling*, US Geological Survey Open File Report 2004-1068, 64 pp., 2004.
- Wertz, F., F. Gherardi, P. Blanc, A.G. Bader, and A. Fabbri, Modeling CO<sub>2</sub>-driven cement alteration at well-caprock interface. Submitted to TOUGH Symposium 2012 Proceedings.
- Xu, T., E.L. Sonnenthal, N. Spycher, and K. Pruess, TOUGHREACT - A simulation program for non-isothermal multiphase reactive geochemical transport in variably saturated geologic media: Applications to geothermal injectivity and CO<sub>2</sub> geological sequestration. *Comp. & Geosc.* 32, 145-165, 2006.
- Xu, T., E. Sonnenthal, N. Spycher, and K. Pruess. *TOUGHREACT User's Guide: A Simulation Program for Non-isothermal Multiphase Reactive Geochemical Transport in Variably Saturated Geologic Media*, Report LBNL-55460, Lawrence Berkeley National Laboratory, Berkeley, Calif., 2004.
- Xu, T., and K. Pruess, Modeling multiphase non-isothermal fluid flow and reactive geochemical transport in variably saturated fractured rocks: 1. Methodology. *Am. J. Sci.* 301, 16-33, 2001.